HPHT synthesis of highly doped InxCo4Sb12 – Experimental and theoretical study

Juliusz Leszczyński, Wojciech Szczypka, Christophe Candolfi, Anne Dauscher, Bertrand Lenoir, Andrzej Koleżyński

HPHT synthesis of highly doped $In_xCo_4Sb_{12}$ – experimental and theoretical study

Juliusz Leszczyński[1 *], Wojciech Szczypka[1], Christophe Candolfi[2], Anne Dauscher[2], Bertrand Lenoir[2] and Andrzej Koleżyński[1]

[1] *Faculty of Materials Science and Ceramics, AGH University of Science and Technology, Al. Mickiewicza 30, 30-059 Cracow, Poland*

[2] *Matériaux à propriétés thermoélectriques, Institut Jean Lamour, CP2S Parc de Saurupt, CS 50840 UMR 7198 CNRS - Université Lorraine 54011 Nancy Cedex - France*

[*] *e-mail: juliusz.leszczynski@agh.edu.pl*

Abstract

Indium-filled skutterudite $In_xCo_4Sb_{12}$ with high filling fraction x (above the solubility limit) was synthesized using HPHT synthesis method. Obtained samples were characterized by means of XRD with Rietveld structural refinement and XPS methods, confirming the introduction of indium filler into structural voids in much higher concentration than solubility limit in ambient conditions. The electrical and thermal properties measurements carried out for temperature range of 4-300 K showed increased carrier concentration and simultaneously decreased Seebeck coefficient and thermal conductivity. Additionally, DFT calculations for $In_xCo_4Sb_{12}$ (x = 0, 0.125, 0.25, …, 1) were carried out employing PBE and modified Becke-Johnson (mBJ) exchange-correlation potentials. Analysis of calculated band structures indicated that increase of In content in $CoSb_3$ voids results in significant decrease of band gap size due to down-energy shift of conduction band at H point of first Brillouin zone. Net charges of topological atoms calculated within QTAiM model were found to be consistent with tendencies observed in XPS measurements. The obtained results show that using HPHT synthesis method allowed obtaining materials with filler element concentration being much higher than solubility limit in ambient conditions and therefore modifying the structure of skutterudite materials (and thus its thermoelectric properties) to a larger extent.

Keywords

- skutterudites
- HPHT
- WIEN2k DFT calculations
- electronic structure
- Bader's QTAiM analysis

Introduction

Skutterudites are one of the best mid-temperature range thermoelectric materials for thermoelectric applications in power generation. Optimization of their thermoelectric performances was possible due to their remarkable ability to accommodate various dopants in either the structural voids or in substitution on the framework elements. Among them, indium as a filling element is one of the best dopant to achieve *n*-type $CoSb_3$ thermoelectric material yielding high thermopower α, low electrical resistivity ρ and low thermal conductivity κ. As a result, $ZT = \alpha^2 T/\rho\kappa$ values as high as 1.5 can be reached around 800 K [1].

Crystal structure of skutterudites can be described in many ways. Taking $CoSb_6$ octahedra as the basic group/element of the structure it can be described as a distorted ReO_3 structure composed of corner sharing $CoSb_6$ groups, where four of the neighboring octahedrons are distorted and tilted to form Sb_4 rings. However, contrary to ReO_3 chemical bonding in skutterudite cannot be defined only through $CoSb_6$ octahedra, but Sb-Sb bonds inside the Sb_4 ring are crucial for structural stability and for transport properties. Rapprochement of the Sb corners of the octahedrons creates dodecahedral voids a very important feature of this structure, where guest atoms can be placed.

Both undoped as well as variety of partially or fully filled $CoSb_3$ were analyzed theoretically within DFT calculations in a last decade. Hammerschmidt *et al.* [2] examined pure $CoSb_3$ using a set of popular DFT exchange-correlations potentials. Results obtained employing PBE-GGA potential indicated reasonable agreement with the experiment when comparing bulk moduli and cohesive energies. In the same work, as well as in many other papers [3, 4, 5] authors indicate substantial sensitivity of results of electronic structure calculations due to subtle changes in skutterudite structure (mainly related to positional parameters of Sb atoms). The problem of skutterudite band gap estimation was also examined by Khan *et al.* [6], who indicated modified Becke-Johnson potential [7] as an efficient

potential for electronic structure calculations in skutterudites, especially when implemented in a non-regular form. On the other hand, wide range of experimentally estimated band gap size of $CoSb_3$ which is reported in the literature, leads to arbitrary nature of evaluation of suitability of applied theoretical methods.

Extensive analysis devoted to filled $CoSb_3$ was performed by Hammerschmidt *et al.* [8]. PBE calculations for $Y_xCo_4Sb_{12}$ (Y = Ga, In, Tl) indicated that materials with high filling fractions can exhibit better transport properties than skutterudites with low content of a filler. According to the authors, increase of filler content results in decrease of a band gap and thus increase of power factor.

It was proven that contrary to the primary attempts of electronic structure description Co gains negative charge and Sb gains positive charge. Theoretical results based on electronic band structure calculations are in this matter in very good agreement with experimental XRD results. XPS measurements were used in experimental study of a chemical state of atoms composing the skutterudite framework as well as for the guest atoms and shown their ionic character. For the alkaline and alkaline earth metals as well as for lanthanides it was experimentally and theoretically proved that they create ionic bond with the host framework and the charge transfer is close to their oxidation states. For indium filled skutterudites Zhao *et al.* [9] suggested that indium in the $CoSb_3$ skutterudite structure becomes +1 cation. This is in agreement with our findings based on the experimental results and theoretical calculations [10]. However, Zhao *et al.* in their discussion concerning bonding in the skutterudite structure assumed Co at +3 oxidation state and Sb at -1 what is in contradiction with experimental and theoretical findings in the last years.

Quite a few studies on high pressure high temperature HPHT synthesis of skutterudites were carried out so far. First attempts were devoted to introduction of filler elements into the voids for elements which at normal conditions do not form filled skutterudites (Mg [11]) or in order to increase the void filling fraction (Mm(Mm-mischmetal) [12], Ca [13], Li&Ca [14]). Increase of the filler element concentration, as was shown in several cases can improve thermoelectric properties at higher temperatures through decrease of the intrinsic carriers effects resulting in reduction of Seebeck coefficient. Also, numerous investigations on synthesis of $CoSb_3$ using HPHT method, where substitution on the skutterudite framework was employed to modify material properties, were published. These were studies on dopants such as: Te [15] Se, Se/Te [16], Sn [17] and Fe [18], In and Ge substituted $CoSb_3$ [19]. Many of these research used HPHT conditions in order to shorten the synthesis time rather than to form new compounds with skutterudite structure. The main issue in the case of the new high pressure phases is their metastability. It was shown

for $Sr_xBaCo_4Sb_{12}$ synthesized using high pressure torsion HPT method that annealing at moderately high temperature (673K) or even thermoelectric properties characterization in a temperature range usually used for this type of materials causes withdrawal of structural and microstructural changes induced by high pressure. In some of the research after the HPHT synthesis additional thermal processes, which can decompose the obtained high pressure structure, were used. Thus, it is highly probable that the studied properties were corresponding to ambient pressure equilibrium phases or to some intermediate state. The HPHT synthesis of indium filled $CoSb_3$ was investigated by Deng and coworkers, however, the nominal filling fraction of voids was limited to $x = 0.4$ [20] a value close to a filling fraction limit under ambient pressure. They have studied the properties only at and above the room temperature for samples prepared at different pressure, finding that the one obtained at the lowest pressure possessed best thermoelectric properties.

In this paper, we present results of our attempts to synthesize material completely filled with In using HPHT conditions, in order to examine the In filling fraction limit under high pressure and influence of indium content on the thermal conductivity. Another goal of this study was to examine the indium chemical state in the skutterudite structure using XPS method, what should be facilitated by increased In concentration, and to compare the electronic transport properties from 4K up to 350K with a sample obtained at ambient pressure having nominal composition $In_{0.4}Co_4Sb_{12}$. The experimental study is supported by DFT band structure calculations and analysis of electronic charge density topology as well as by comparison of transport properties calculated using BoltzTraP software compared with the experimental results.

Experimental details

Synthesis

The $InCo_4Sb_{12}$ material was prepared by direct reaction of a stoichiometric mixture of pure elements. Preparation of In filled cobalt triantimonide samples at ambient pressure has been reported in our previous work [10]. The first synthesis steps of the material obtained at HPHT conditions were similar to those used for the samples obtained at ambient pressure. Stoichiometric mixture of pure elemental In (shots 99.999%), Co (powder 99.95%) and Sb (ingot 99.99%) was enclosed in evacuated quartz tube, heated at 970°C for 3h, cooled down and kept at 700°C for 12 h. After that, the obtained ingot was ground into powder in an agate mortar and placed in combined graphite-pyrophilite die in a high pressure Bridgeman type press. Synthesis lasted 3 minutes at 700°C at 7.5GPa. The result

was fractured sample having a diameter of 15 mm and a height of 4 mm. Specimens for further measurements were cut using a diamond disc saw.

Measurements

The XRD measurements were performed on pulverized sample after HPHT synthesis using $Cu_{K\alpha 1}$ wavelength (Empyrean diffractometer, Ge(111) monochromator). Transport property measurements were carried out on a bar-shaped sample 2x2x10 mm. Electrical resistivity, Seebeck coefficient and thermal conductivity were simultaneously measured between 2 and 350 K using the thermal transport option (TTO) of a physical property measurement system (PPMS, Quantum Design). Hall effect measurements were performed by a five-contact method. For more details we refer to the previous paper [10]. Photoelectron spectroscopy XPS was used for chemical analysis of the bulk sample surface. XPS measurements were carried out using VSW (Vacuum Systems Workshop Ltd. England) apparatus. X-ray source was an Al anode lamp rated at 210W, using Kα line 1486.6 eV with angle of incidence 15°. Photoelectron energy was analyzed using hemispherical analyzer with 150 mm radius working in fixed analyzer transmission mode, equipped in 18-channel two-plate Galileo detector working at 1.8 kV. The electron energies were calibrated using C-C and C-H bonds energy of 284.6 eV as a reference.

Computational details

The electronic structure calculations for $In_xCo_4Sb_{12}$ structures (x = 0, 0.125, …, 1) have been carried out by means of WIEN2k FP-LAPW package within Density Functional Theory formalism [21, 22, 23, 24]. The following parameters have been chosen for calculation: 400 k-points (7x7x7 mesh within the irreducible Brillouin zone) for simple crystal cells and 50 k-points (3x3x3 mesh) for 2x2x2 supercells, cut-off parameter Rk_{max} = 7.5, GGA-PBE exchange-correlation potential [25], the values of muffin-tin radii (R_i) [a.u.]: Co - 2.27, Sb - 2.27, In - 2.27 and the convergence criteria for SCF calculations set to $\Delta E_{SCF} \leq 10^{-5}$ Ry for total energy and $\Delta \rho_{SCF} \leq 10^{-5}$ e for electron density topology analysis. For all structures full optimization of crystal cell volume and atomic positions was performed and band structures were calculated for selected path consisted of a high symmetry points in reciprocal lattice for respective unit cells as defined on Bilbao Crystallographic Server **http://www.crst.ehu.es** [26]. Additional calculations of band structures employing modified Becke-Johnson (mBJ) potential [7] (known for giving improved band gaps for semiconductors) were carried out.

Results obtained from WIEN2k calculations with dense k-meshes (96000 k-points for simple unit cells and 12000 k-points for supercells) were used to determine transport properties from Boltzmann theory of transport implemented in BoltzTraP [27] program. In order to provide reliable and comparable analysis BoltzTraP calculations were performed using densities of states obtained by applying mBJ potential.

Topological analysis of total electron density distribution in optimized structures was performed within Bader's Quantum Theory of Atoms in Molecules (QTAiM) [28] using Critic2 program [29].

Results

XRD

Fig. 1 shows XRD patterns in the low 2θ range for a pre-reacted $InCo_4Sb_{12}$, $InCo_4Sb_{12}$ sample after high pressure synthesis and $In_{0.4}Co_4Sb_{12}$ sample for comparison. The pre-reacted sample consists mainly of skutterudite phase with InSb and $CoSb_2$ impurities being a result of exceeding of the In solubility limit in $CoSb_3$. After HP treatment amount of the impurities decreases significantly indicating the incorporation of indium to skutterudite structure. Simultaneously, reflections (*e.g.* (130)) are shifted toward lower angles corresponding to lattice parameter increase accompanied by extinction of the (110) and (200) reflections resulting from filling of the structural voids. In **Fig. 2** results of the Rietveld refinement of the $InCo_4Sb_{12}$ diffraction pattern are presented. Detailed analysis showed that after HP synthesis, beside the presence of InSb and $CoSb_2$ impurities a minute amounts of In can be also found. The experimental data can be quite well fitted with the theoretical model (**Table 1**; the limiting factor of a better fit is the specimen quality). Careful observation of skutterudite phase peaks shows that they can be composed of two highly overlapping peaks corresponding to two skutterudite phases with very similar lattice parameter. Surprisingly the Oftedal relationship 2(y+z)=1 is not as good fulfilled as in $CoSb_3$ but better than in $In_{0.4}Co_4Sb_{12}$. For the calculated In occupation parameter $In_{0.78}Co_4Sb_{12}$ formula can be proposed. As for all of the cobalt triantimonide skutterudites it can be clearly seen that the void radius compared with the indium cation radius is substantially larger (r_{void}=197.3 pm, r_{In}^{+}=104 pm, r_{In}^{3+}=81 pm). This feature allows significantly greater movement of the guest atoms as compared to that of the framework atoms. These vibrations can be measured as the mean square displacement of the atom which can be determined in XRD diffraction experiments as the atomic displacement parameter (ADP). The ADP of the In as it was determined in previous study for $In_xCo_4Sb_{12}$ is significantly larger compared to the host Sb and Co atoms confirming large freedom of movement of the filler element. The lattice constant at 300K for $InCo_4Sb_{12}$ is

a = 9.11497 Å. The increase of the lattice parameter (**Fig. 3**) is significantly higher than predicted from linear fit for lower In filling fractions, determined in our previous study using electron probe microanalysis (EPMA) [10]. This discrepancy can be a result of lattice expansion caused by introduction of other than In atoms into the voids *e.g.* Sb. However, the XPS results do not give any clear indication of chemical state of Sb corresponding to void filling by Sb, nevertheless it cannot be excluded.

On the other hand, the measured lattice parameter match fairly well a linear fit of experimental data of Visnow *et al.* [30] who estimated the In content based on Rietveld refinement of neutron diffraction results, thus the observed discrepancy can have origin in In content determination method. Moreover, in the work of Sekine *et al.* [12] for a fully filled by mischmetal $CoSb_3$ (synthesized at 4.5 GPa) a lattice parameter slightly higher than 9.10 Å was observed, which corresponds well with our result of the lattice constant. Unfortunately, neither in the Sekine nor in the Yang, Li and Deng papers the presented powder XRD results shows 2θ range below 20°, where the (110) and (200) reflection can be observed, which should diminish upon increasing filling fraction of the structural voids. The overall slope of the lattice parameter dependence on indium content is well reproduced in theoretical calculations. While comparing the lattice parameter to Dong results on HPHT synthesized $In_{0.4}Co_4Sb_{12}$ (**Fig. 3**) one can see in their study a surprisingly strong dependence of the lattice constant on the synthesis pressure, not observed in other research *i.e.* Zhang HPHT $CoSb_{3-x}Te_x$ vs. Wojciechowski [31] $CoSb_{3-x}Te_x$ (for $CoSb_{2.5}Te_{0.5}$ 0.9048 Å HPHT vs. 9.0487(5) Å for non-HPHT) or in earlier mentioned Sekine (for $Mm_{0.2}Co_4Sb_{12}$ $a \cong 9.052$ Å (HPHT) vs. 9.0565 Å [32]). Moreover, an opposite effect on the lattice parameter was observed in a paper of Rogl *et al.* [33] where use of high pressure torsion HPT method resulted in increase of the lattice parameter of $Sr_{0.07}Ba_{0.07}Yb_{0.07}Co_4Sb_{12}$ from 9.057 to 9.082 Å, which could be ascribed to an enhanced dislocation density, additional grain boundaries and a smaller crystallite size which were observed for the HPT processed samples.

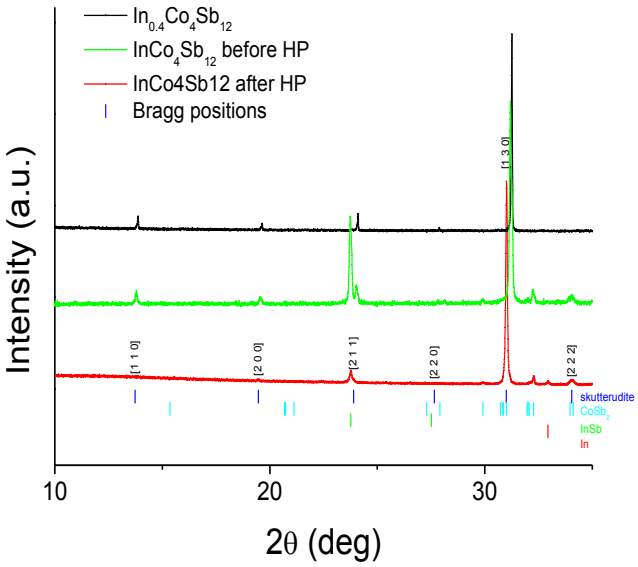

Fig. 1 XRD patterns of $In_{0.4}Co_4Sb_{12}$ and $In_1Co_4Sb_{12}$ before and after HPHT processing.

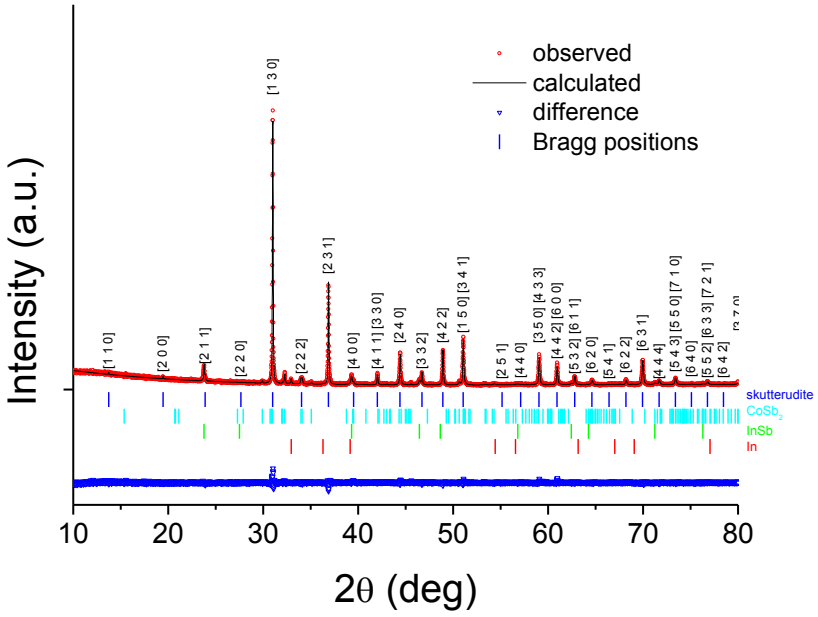

Fig. 2 XRD patterns of HPHT synthesized $InCo_4Sb_{12}$.

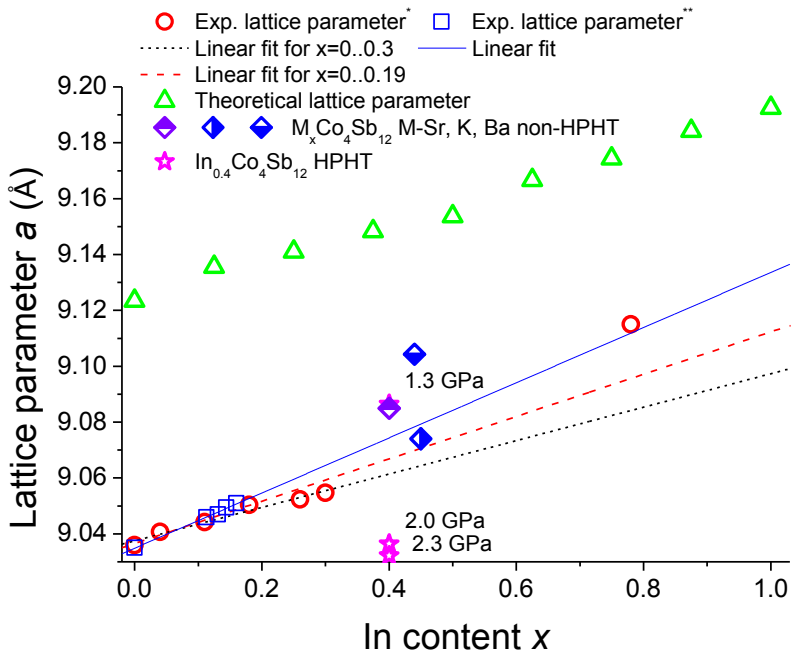

Fig. 3 Dependence of lattice parameter on In filling fraction *x* determined from XRD measurements (circles) (this work and [10]) and calculated in DFT calculations (triangles) for $In_xCo_4Sb_{12}$. For comparison, experimental results of the lattice parameter of $In_xCo_4Sb_{12}$ presented by Visnow *et al.* [30] for non-HPHT $In_xCo_4Sb_{12}$ (boxes) and by Deng *et al.* [20] for $In_{0.4}Co_4Sb_{12}$ obtained under different pressure by HPHT method (asterisks), are shown, as well as values of the lattice parameters for K-[34], Sr-[35], and Ba-[36] filled $CoSb_3$. In order to facilitate readability of the plot, linear dependences of the lattice parameter on the In filling fraction are drawn as dash and solid lines.

Table 1 Rietveld refinement of powder XRD for $InCo_4Sb_{12}$ HPHT sample.

Rietveld refinement goodness of fit parameters:						
	R_p: 32.6	R_{wp}: 21.6	R_e: 18.4	Chi^2: 1.379		
Atom	Wyckoff position	x	y	z	B_{iso}	site occupancy
Sb	24g	0.1583(15)	0.3363(13)	0.00000	0.49(3)	0.993(13)
Co	8c	0.25000	0.25000	0.25000	0.4(15)	1.00000
In	2a	0.00000	0.00000	0.00000	1.18(13)	0.78(12)
Lattice constant (Å) 9.11497(3)						
Quantitative analysis						
Phase	Faction(%)		Rf-factor			
$InCo_4Sb_{12}$	82.51(2.88)		5.06			
$CoSb_2$	9.62(0.29)		12			
InSb	6.36(0.16)		7.70			
In	1.51(0.07)		10.8			

XPS

Fig. 4 shows photoemission spectra of In $3d_{5/2}$ for $InCo_4Sb_{12}$, $In_{0.4}Co_4Sb_{12}$, InSb and In samples. It can be observed that In $3d_{5/2}$ peak energy is shifted toward higher energy in the skutterudite structure compared to metallic In and InSb meaning that In is transferring their electrons to the $CoSb_3$ framework. However, the chemical shift for indium

is relatively small suggesting that it is at +1 oxidation state with $[Kr]4d^{10}5s^2$ electron configuration. This is in agreement with our previous band structure calculations using KKR method [10] and with the presented here QTAIM topological atom net charge. The same value of In oxidation state proposed Zhao *et al.* [9] based on a chemical shift of two Sb $3d_{5/2}$ peaks and later [37] based on BS calculations and XANES results. For $InCo_4Sb_{12}$ where the saturation of the skutterudite framework with electrons donated by the "guest" is higher, the effective charge transfer between In and the framework is decreased, reflected by reduced chemical shift of In $3d_{5/2}$ peak. The In $3d_{5/2}$and $3d_{3/2}$ energy levels are not split suggesting that indium occupies central position of the structural void. This is in agreement with our previous x-ray and neutron diffraction results and with K-edge XANES study findings of Zhao *et al.* [37].

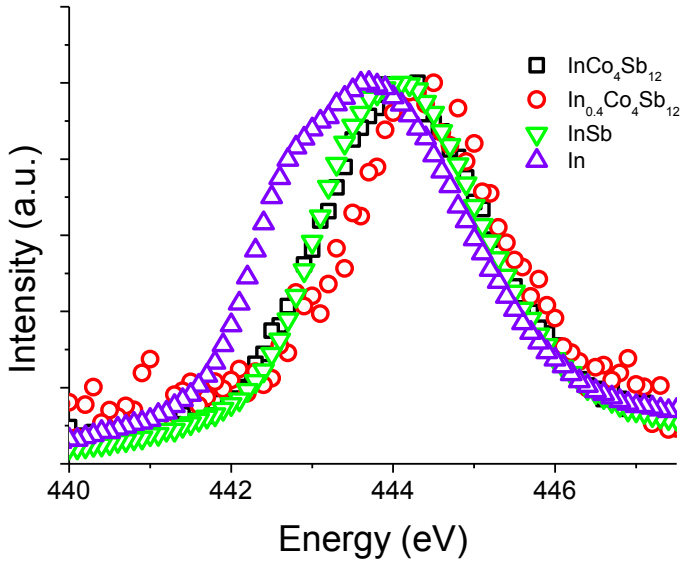

Fig. 4 XPS spectra of In_{3d} energy level in $In_{0.4}Co_4Sb_{12}$, $InCo_4Sb_{12}$ and reference materials In and InSb.

Table 2 XPS measurement results for selected energy levels.

	Sample			
Energy level	$InCo_4Sb_{12}$	$In_{0.4}Co_4Sb_{12}$	InSb	In
In $3d_{5/2}$ (eV)	444.26	444.40	444.1	443.84
In $3d_{3/2}$ (eV)			451.69	451.34
In MNN (eV)	-	-	1077.22	1075.20
	-	-	1079.87	1078.00
	-	-	1085.28	1085.28
				Sb*
Sb $3d_{5/2}$ (eV)	527.19	527.48	527.17	528.21
	529.23	529.4	529.71	
Sb $3d_{3/2}$ (eV)	536.63	536.95	536.61	538.00
	538.72	539.08	539.25	
Sb MNN (eV)	1021.43	1022.65	1021.86	-
	1031.30	1031.70	1031.42	-
				Co*
Co $2p_{3/2}$ (eV)	777.39/778.77	777.88/780.31	-	777.90 – 778.3
Co $2p_{1/2}$ (eV)	792.42	792.75	-	793.3

*Energy levels for pure Sb and Co are taken from NIST database.

The remaining results of XPS measurements are summarized in **Table 2.** The Sb $3d_{5/2}$ and $3d_{3/2}$ peaks (**Fig. S1** in Electronic Supplementary Materials) are split into two main peaks which can be attributed to Sb-Sb and Co-Sb bonds with binding energy slightly lower compared to energy of pure Sb for the former and higher for the latter. Also, for other recorded Sb peaks (Auger MNN, **Fig. S2**), splitting into two binding energies is observed with similar binding energy shift. The general picture of the Sb 3d level spectra for both skutterudite samples is similar, showing no extra peaks which could correspond to Sb atoms placed inside the icosahedral void. Shift of Sb 3d energy level corresponding to Co-Sb bond is towards higher energy which is equivalent to an increase of positive charge at Sb. Of course, other than the two main peaks can be fitted to the $3d_{5/2}$ and $3d_{5/2}$ photoelectron spectra and they can be assigned to various Sb bond types and/or Sb in different chemical state as it was done by Tang *et al.* [38] and Zhao *et al.* [9]. However, in our opinion, assignment of peaks obtained through the photoemission spectra decomposition should be done with great care and linked with complementary measurements, for otherwise it would be just speculation, therefore we do not discuss these results in a more detailed manner. For Co photoemission spectra $2p_{1/2}$ and $2p_{3/2}$ energy levels show two chemical states overlapped by Co 2p and Sb 3p energy loss peaks (**Fig. S3**). This result is different from Tang [38] and Zhao measurements who observed single or strongly overlapped peaks of Co 2p energy levels. Unfortunately, they did not performed fit of the Co 2p spectra and it is impossible to unambiguously judge their results. However, for the Co LMM Auger kinetic energy spectra (**Fig. S4**) we could fit it with two overlapping peaks looking similar to the results of Tang and Zhao. Contrary to the Zhao observations for

lower In filling fraction of $CoSb_3$, with the increasing amount of In the Co 2p peaks are moved toward lower energy which corresponds well with increasing negative charge collected at Co upon In doping.

Transport measurements

As it was shown in several papers before, insertion of In into the structural voids changes the p-type semiconducting $CoSb_3$ in n-type semiconductor. This is reflected in the negative sign of thermopower in the whole temperature range from 2 to 300 K (**Fig. 5**). The absolute value of thermopower is lower for the $InCo_4Sb_{12}$ HPHT sample than for the $In_{0.4}Co_4Sb_{12}$ sample and increases almost linearly with temperature, which is characteristic for highly doped semiconductors. Temperature dependence of electrical resistivity for $InCo_4Sb_{12}$ at low temperatures is different from metallic like dependence of $In_{0.4}Co_4Sb_{12}$ (**Fig. 6**). The resistivity increases with temperature up to about 150 K and then begins to decrease. Surprisingly, the electrical resistivity at the whole analyzed temperature range is greater than for the sample with the maximum filling fraction synthesized at atmospheric pressure. In the work of Deng [20] it was reported that for the same initial sample composition the observed electrical resistivity increased slightly with the increase of the synthesis pressure despite increasing carrier concentration. To get deeper insight to electrical properties, Hall effect measurements were carried out, assuming single parabolic band model. Hall effect measurement results show that the obtained sample has a very high carrier concentration range of $n = 1.1 \cdot 10^{21}$ cm^{-3} *i.e.* about 4 times greater than the $In_{0.4}Co_4Sb_{12}$ sample (actual indium content x = 0.26) which corresponds to nearly four times higher indium content. The predominant type of charge carriers are electrons. Hall carrier concentration at low temperatures (**Fig. 7**) is rising to about 130 K achieving the maximum and then decreases. The mobility of carriers is very low and at 300 K is 4 $cm^2/V/s$ which is a value almost ten times lower than for $In_{0.4}Co_4Sb_{12}$ and close to the value of mobility in completely filled *p*-type skutterudites or in Ca partially filled $CoSb_3$ [39]. Temperature dependence of mobility has complex character: it falls to about 130 K to reach a growing trend, likewise, the atypical nature of a dependence of the Hall constant. Similar temperature dependence of the Hall constant was observed for $NaFe_4Sb_{12}$ and KFe_4Sb_{12} [40] where the anomalies *i.e.* rise of the R_H were explained by ferromagnetic ordering. Electrical resistivity dependence is similar below 120 K to fully filled iron antimony skutterudites but the resistivity decrease above 150 K is unusual. This is not the case of our material as for the other transport properties we observe different behavior than Schnelle *et al.* These effects can be a result of hole minority carriers generated by excitation of electrons through a narrow band gap. These features observed at Hall constant R_H and mobility dependence corresponds to thermopower dependence where a small hump at about 150 K is present and for higher temperatures

the increase of the Seebeck coefficient is still linear but less steep. Using approach and equations presented in [41] carrier effective mass was calculated to be in the range of 1.99 and 5.81 m_e between 2 and 300 K. Impact of the HPHT synthesis on electrical resistivity of polycrystalline materials is complex. On the one hand, high pressure conditions can reduce resistivity trough reduction of porosity and increase of material density, but on the other hand it can introduce several types of point, linear and planar defects and thus strains to material, resulting in increased resistivity. Increased electrical resistivity for HPT samples of $Sr_{0.07}Ba_{0.07}Yb_{0.07}Co_4Sb_{12}$ was reported by Rogl *et al.* [33]. A minute increase of resistivity was also shown by Deng [20] between samples prepared at high pressure (1.3 – 2.3 GPa). More significant increase is visible when we compare their results for $In_xCo_4Sb_{12}$ samples (x = 0.1 and 0.3: $\rho_{(300K)} \cong 80$ μΩ·m) to samples prepared under non HPHT conditions (for x = 0.26: $\rho_{(300K)} = 8$ μΩ·m [10]), however, much lower carrier concentration is observed in Deng's samples what is corroborated by higher absolute values of Seebeck coefficient. Very similar difference between the resistance of the HPHT and non HPHT sample can be observed between Sekine [12] and Rogl [32] samples, where for HPHT $Mm_{0.4}Co_4Sb_{12}$ $\rho_{(300K)} \cong 47$ μΩ·m and for non HPHT $Mm_{0.35}Co_4Sb_{12}$ $\rho_{(300K)} \cong 4$ μΩ·m. Opposite impact of high pressure can be shown for example in Te doped $CoSb_3$. For $CoSb_{2.7}Te_{0.3}$ obtained in HPHT conditions [15] the resistivity is lower $\rho_{(300K)} = 7.6$ μΩ·m compared to the same composition in paper of Wojciechowski *et al.* [31] where resistivity $\rho_{(300K)} = 7.7$ μΩ·m but at slightly higher carrier concentration ($n = 3.5 \cdot 10^{20}$ vs. $4.5 \cdot 10^{20}$ cm^{-3}) and lower absolute Seebeck coefficient ($S = -147$ μV/K vs. -117 μV/K). In case of our study the observed resistivity increase is quite remarkable, similar to those reported by Sekine, suggesting strong impact of defects and stress generated by high pressure on the resistivity.

Thermal conductivity

Temperature dependence of the lattice contribution to the thermal conductivity of $In_{0.4}Co_4Sb_{12}$ and $InCo_4Sb_{12}$ samples is presented in **Fig. 8**. Lattice thermal conductivity of $In_{0.4}Co_4Sb_{12}$ sample is typical for polycrystalline material, with a maximum at 50 K, however the maximum value is strongly suppressed compared to unfilled $CoSb_3$. The lattice thermal conductivity of the $InCo_4Sb_{12}$ sample is slightly different as the conductivity does not reach a maximum but increases with temperature up to temperature 80 K and then remains almost constant. This result is very similar to findings of Sekine *et al.* for $Mm_xCo_4Sb_{12}$ [12]. For whole temperature range the thermal conductivity of the $InCo_4Sb_{12}$ sample is much lower compared to the $In_{0.4}Co_4Sb_{12}$ sample. Compared to results of Deng the thermal conductivity at 300 K is two times lower. In order to explain the origin of the increased phonon scattering a Callaway model of the lattice thermal conductivity was fitted to the experimental data (**Fig. 8**). It was possible to find

good correlation of the fitted model to the experiment, however, very similar goodness of fit was obtained for parameters' sets where the scattering factor varied in a wide range, making them useless for drawing any conclusions on the dominant phonon scattering mechanism. Significantly reduced thermal conductivity of the $InCo_4Sb_{12}$ sample shows that the phonon scattering processes, due to the higher In ions concentration as well as the higher disorder and/or perhaps strain, are much stronger compared to the $In_{0.4}Co_4Sb_{12}$ sample. From this point of view increased insertion of In ions by using high pressure have positive effect on thermoelectric properties. Likewise for electrical resistivity, the HPHT synthesis can have different impact on the thermal conductivity. In case of Deng's results thermal conductivity is increased compared to non-HPHT samples [10]. However, in most cases HPHT process reduce the thermal conductivity like in case of Mm Rogl (HPT) [33] or Ca filled samples [13, 42]

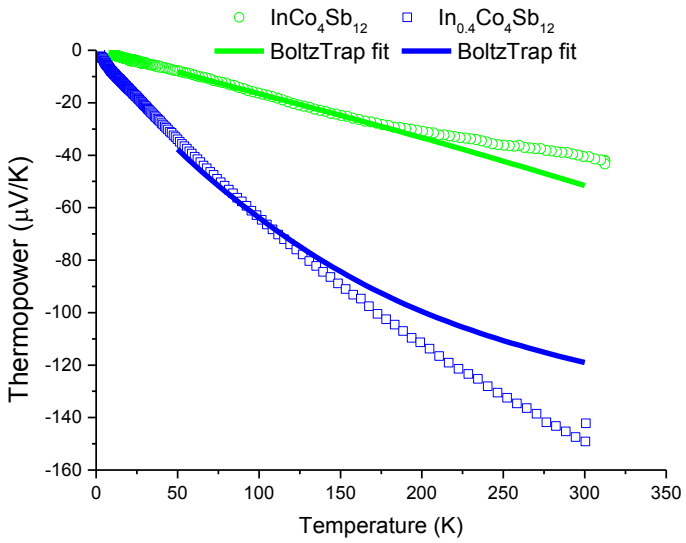

Fig. 5 Temperature dependence of the Seebeck coefficient for $In_xCo_4Sb_{12}$. Solid lines present BoltzTraP fitting results described later in the text.

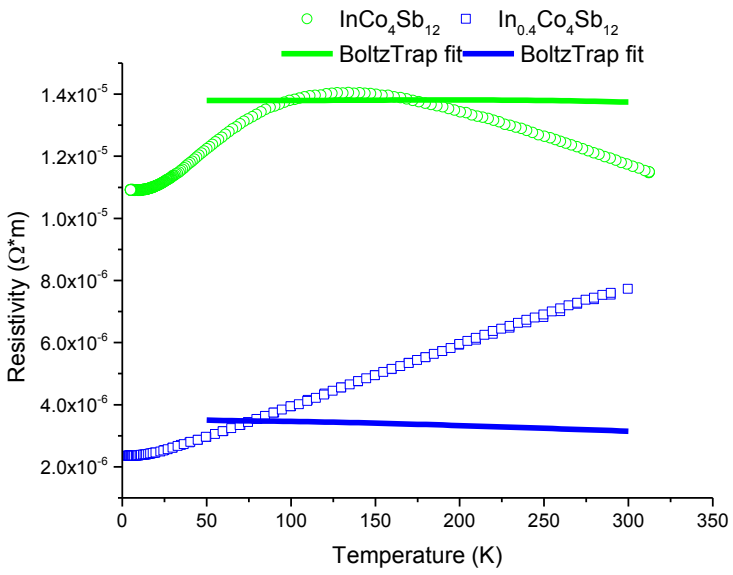

Fig. 6 Temperature dependence of the electrical resistivity for $In_xCo_4Sb_{12}$. Solid lines present BoltzTraP fitting results described later in the text.

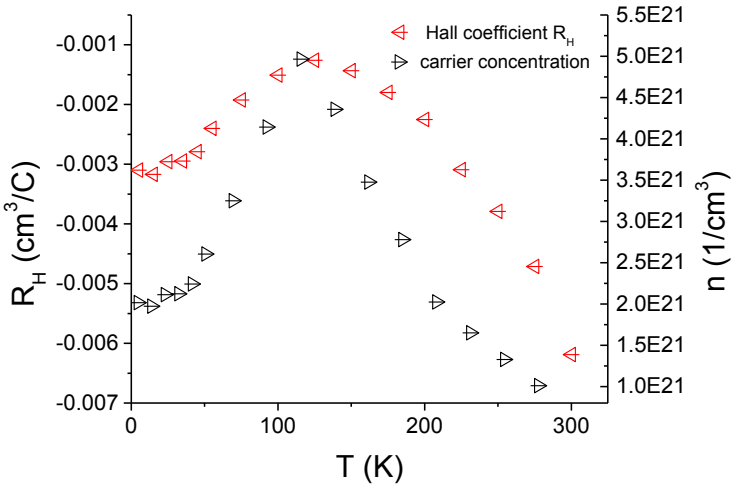

Fig. 7 Temperature dependence of the Hall coefficient R_H and hall carrier concentration *n* for $InCo_4Sb_{12}$.

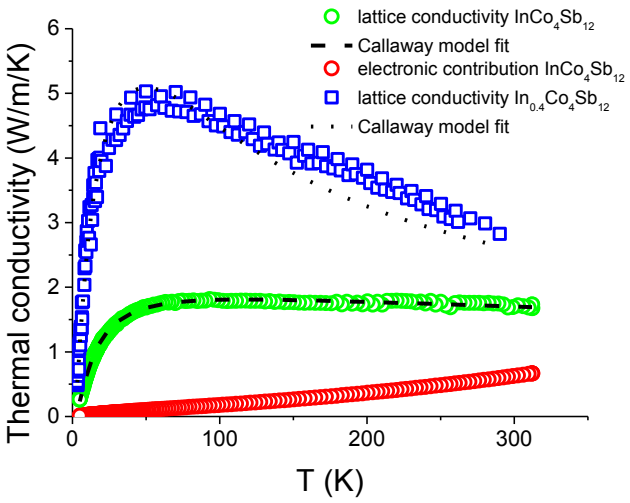

Fig. 8 Temperature dependence of the thermal conductivity for $In_{0.4}Co_4Sb_{12}$ and $InCo_4Sb_{12}$ fitted with a Callaway model (more detailed description in the text).

Electronic structure

Due to generally poor reproducibility of experimental band gap measurements in DFT calculations carried out using PBE potential, more accurate mBJ potential is applied often in calculations for thermoelectric materials [43, 44, 45]. In **Fig. 9** band structures of pristine Co_4Sb_{12} and filled $InCo_4Sb_{12}$ are presented. The former structure exhibits direct band gap at Γ point with size ca. 370 meV. A second conduction band (CB) minimum belonging to a flat valley is located at H point and lies 75 meV above the minimum at Γ point. This minimum significantly shifts towards lower energy with increasing content of indium introduced to the skutterudite voids and for $x \geq 0.375$ in $In_xCo_4Sb_{12}$ band gap becomes indirect. It is worth to notice that although CB valley around H point mainly exhibits Co *d*-states character, indium states contribution is also significant, as it is shown in the **Fig. 9 b**.

Introduction of indium into $CoSb_3$ voids results in shift of Fermi level towards CB (the higher amount of indium the greater shift) so this material exhibits *n*-type character. Bands in a CB near H point are significantly more flat than in the neighborhood of Γ point, what results in much higher effective mass of conducting electrons in this material, when H point is a minimum of CB. Therefore, change of a band gap character from a direct to an indirect one causes appearance of much more heavy fermions in CB, what might have a significant effect on conductivity in this material.

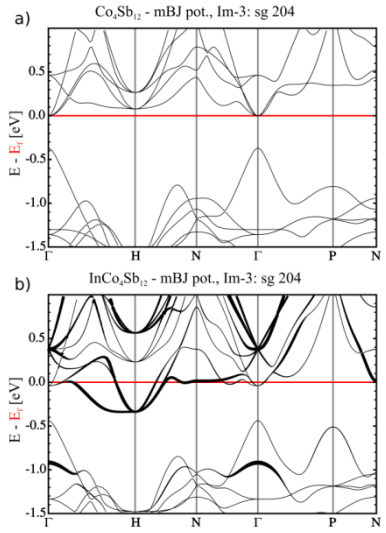

Fig. 9 Band structures of undoped $CoSb_3$ (a) and filled with indium $InCo_4Sb_{12}$ (b), calculated using modified Becke-Johnson potential. In (b) indium character projected on every band is indicated by line thickness.

Another important property of an electronic structure of In-filled $CoSb_3$ is a size of a band gap. Comparison of the results obtained using PBE potential (presented in the **Fig. 10**) suggests that there is a negligible change of a E_g size, except change of a band gap type from direct to indirect (as the CB minimum at H point also shifts towards lower energy, similarly to results of mBJ calculations). Significantly different trend is observed when mBJ calculations are compared. Much higher energy gap is observed for lower amounts of indium ($x \leq 0.25$), but after gap type change to indirect, band gap decreases strongly with increasing filler content, reaching even smaller values than in PBE calculations for $x = 0.875$ and 1.

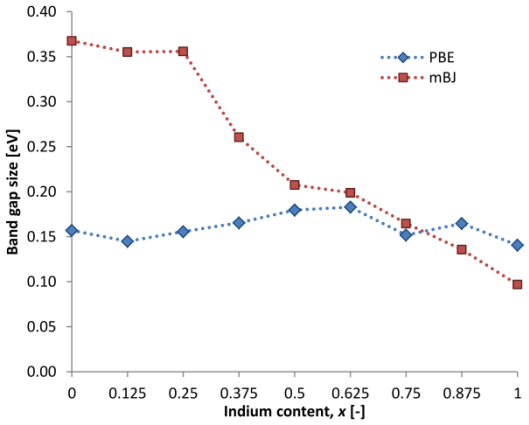

Fig. 10 Relationship between indium content in $In_xCo_4Sb_{12}$ and size of a band gap E_g, obtained using two different potentials: PBE-GGA and modified Becke-Johnson.

Boltzmann transport properties

Calculations of transport properties of $In_xCo_4Sb_{12}$ with various x were carried out using BoltzTraP software in order to undoubtedly check, simultaneously via theoretical and experimental analysis, whether it is possible to significantly improve thermoelectric properties of In-filled cobalt triantimonide, when the amount of introduced indium is much higher than its solubility limit in $CoSb_3$ at ambient pressure conditions.

In the **Fig. 11** results for different compositions of $In_xCo_4Sb_{12}$ were compared. As BoltzTraP calculations were carried out using densities of states obtained from mBJ calculations, band gap gradual change is reflected in Seebeck coefficient values at extrema of $S(\mu)$ plot – the smaller bad gap is observed, the smaller value of S. With increasing amount of In introduced to voids, value of Seebeck coefficient at Fermi level becomes negative and its absolute value decreases gradually, what is a result of Fermi level shift towards conduction band. Simultaneously, the electrical conductivity with respect to relaxation time τ (not shown in the paper) increases due to the increase of a number of charge carriers. Calculated power factor with respect to τ becomes larger when indium content changes from 0 to 0.5, then decreases for $x > 0.5$.

a) b)

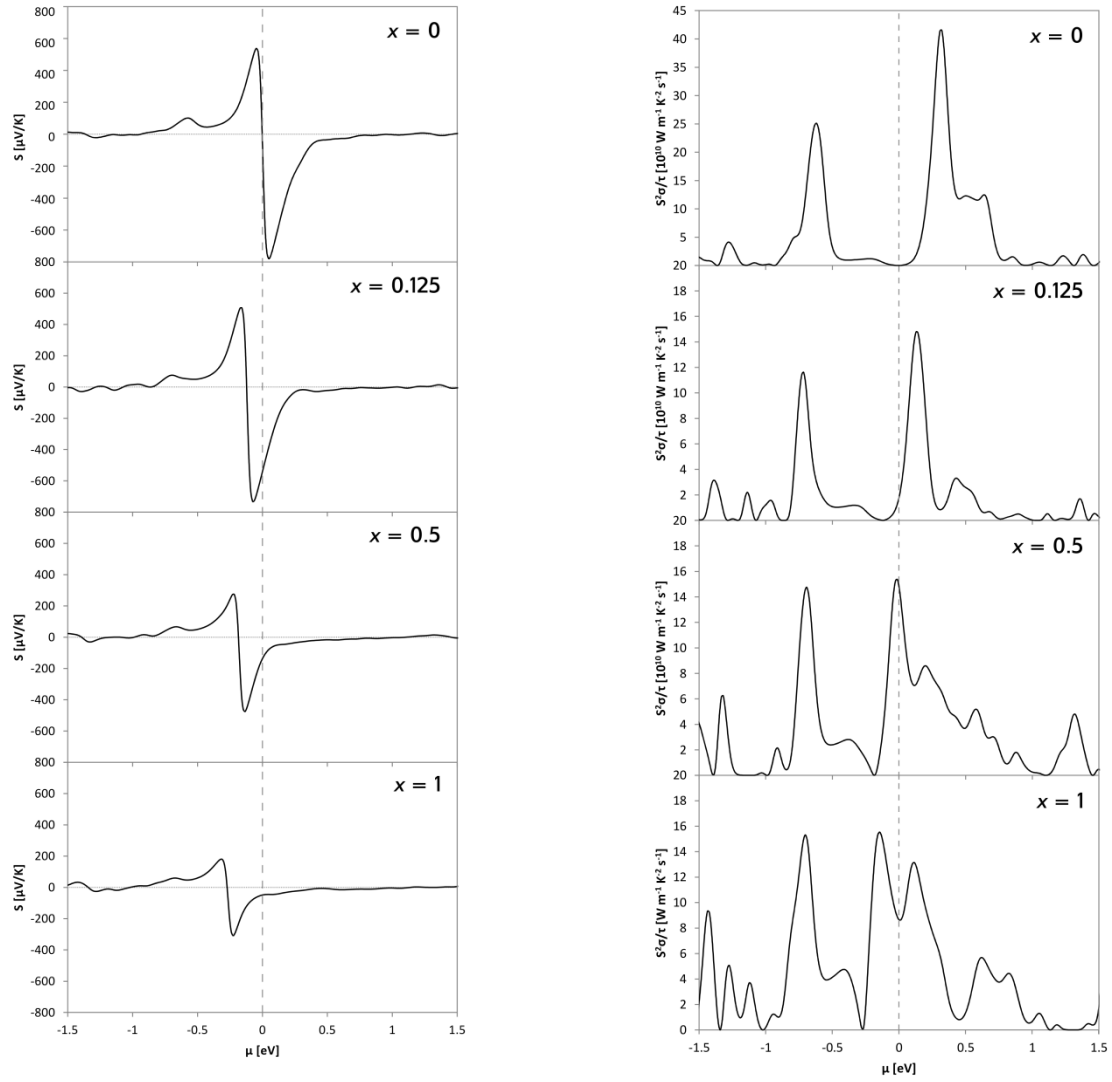

Fig. 11 Seebeck coefficient (S) and power factor ($S^2\sigma$) reduced by relaxation time (τ) for $In_xCo_4Sb_{12}$ with respect to chemical potential (μ) calculated at 300 K.

Due to the fact, that conductivity is relaxation time dependent, it is necessary to adopt τ to be able to compare calculated results with experimental measurements. For an experimental value of Seebeck coefficient (S_{exp}) measured at 100 K chemical potential μ_i was chosen to get $S_{calc}(\mu_i)_{T=100K} = S_{exp}$. For this chemical potential value of σ/τ from calculations and experimental conductivity given at 100 K were read. Calculated τ from $\sigma_{exp}/(\sigma/\tau) = \tau$ was taken as constant in temperature range of experimental measurements. Obtained results are presented in the **Figures 4** and **5**.

Topological properties

Topological analysis of total electron density at bond critical points (BCPs) allows one to define character of bonds present in a crystal structure. BCP is a point of minimum density along a line between two topological atoms, but maximum in both perpendicular directions, where $\nabla\rho(\mathbf{r}) = 0$, and it most accurately reflects the characteristics of the "space" of a chemical bond. The most important properties of BCPs in indium doped $CoSb_3$ structure are presented (for $In_{0.25}Co_4Sb_{12}$ as an example) in the **Table 3**.

Co-Sb bond exhibits the highest value of electron density at BCP and also quite high positive value of Laplacian $\nabla^2\rho(\mathbf{r})$, indicating significant ionic character of these bonds (as $\nabla^2\rho(\mathbf{r}) > 0$ determines closed-shell character of interaction). In case of Sb-Sb bonds value of electron density is still high, depending on particular bond length – the shorter bond length, the higher electron density at BCP. Value of $\nabla^2\rho(\mathbf{r})$ for these bonds is close to zero: negative for shorter bonds and positive for longer ones. Small values of Laplacian indicate a high homogeneity of electron density in the area nearby BCPs of Sb-Sb bonds (especially when value of electron density is high). Therefore, these are not typical of covalent bonds (which exhibit, in general, $\nabla^2\rho(\mathbf{r}) \ll 0$); such configuration of properties of electron density is more of mixed covalent-metallic character of bonding. Much smaller value of electron density together with $\nabla^2\rho(\mathbf{r}) > 0$ at BCP of In-Sb bond indicates that these bonds are very weak and exhibit a closed-shell character. This is a very advantageous feature from the point of view of the phonon glass-electron crystal (PGEC) model. Weak interaction of indium atoms with the rest of the structure results in an increased freedom of movements of these atoms, which may provide better scattering of phonons in the structure.

Comparing the results of QTAiM analysis for structures with various content of indium, only very small changes in bond lengths and properties of total electron density can be observed. In the **Fig. 12,** dependence of bond length (**a**), electron density (**b**) and its Laplacian (**c**) at BCP, respectively, for each bond type, on In content are presented. Shorter Sb-Sb bonds are the most susceptible to an increasing level of void filling by indium atoms, however, even in the case of these bonds, change in bond length between pristine $CoSb_3$ and fully filled $InCo_4Sb_{12}$ is less than 1.5 %. This change affects electron density at BCP and its decrease from 0.36 to 0.34 e/Å^3 is observed. In case of structures with high content of indium, the value of Laplacian of electron density at BCP of these bonds approaches zero.

Table 3 Properties of total electron density at BCPs in $In_{0.25}Co_4Sb_{12}$: d – bond length [Å], $\rho(\mathbf{r})$ – electron density [e Å^{-3}], $\nabla^2\rho(\mathbf{r})$ – Laplacian of electron density [e Å^{-5}], $V(\mathbf{r})$ – potential energy density [a.u.], $H_e(\mathbf{r})$ – electronic energy density [a.u.]. Properties of Sb-Sb bonds have been distinguished between longer bonds (L) and shorter ones (S) in Sb_4 rings.

Bond	d	$\rho(\mathbf{r})$	$\nabla^2\rho(\mathbf{r})$	$V(\mathbf{r})$	$H_e(\mathbf{r})$
In-Sb	1,808	0,116	0,587	-0,031	-0,010
Sb-Sb (L)	1,608	0,304	0,038	-0,360	-0,179
Sb-Sb (S)	1,543	0,352	-0,061	-0,498	-0,245
Co-Sb	1,345	0,408	1,101	-0,388	-0,182

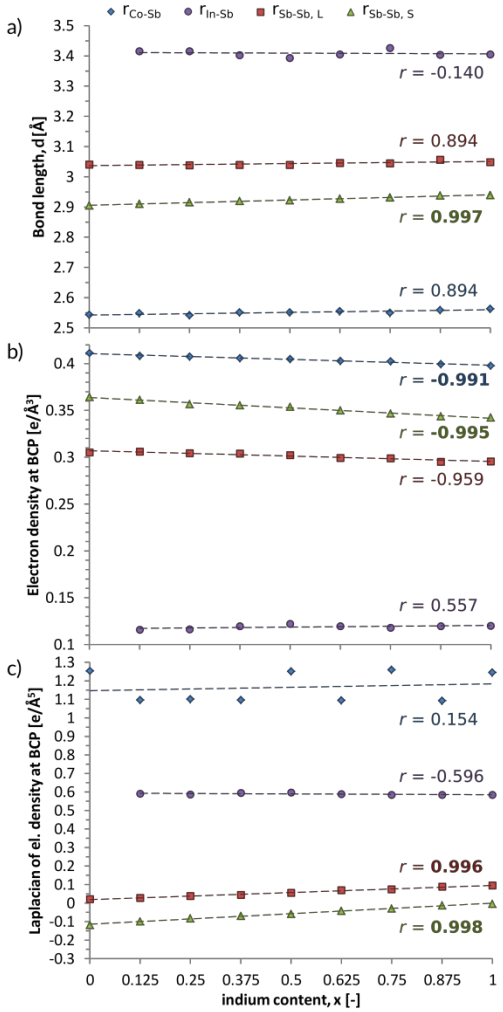

Fig. 12 Average properties of total electron density at BCPs in $In_xCo_4Sb_{12}$: a) bond length [Å], b) electron density [e Å^{-3}], c) Laplacian of electron density [e Å^{-5}], in dependence of indium content. Dashed lines are added as a guide to eyes. Also, for each set of points calculated value of Pearson correlation coefficient r is given.

As the data presented in **Fig. 12** are average values of main types of bonds, some of important details are lost. More detailed information about influence of In proximity on Sb-Sb bonds can be extracted from analysis of local changes

in total electron density. In the **Fig. 13** differential charge density maps provide data on charge density depletion (darkened regions) or accumulation (brightened regions) spaces. Presence of indium in a neighborhood of Sb_4 ring results in a small reduction of charge density, mainly in space between nearest Sb atoms, *i.e.* shorter Sb-Sb bond space. As can be seen in the **Fig. 13 a** this bond is longer than the second short Sb-Sb bond in the Sb_4 ring. Proximity of indium atoms has a little destabilizing effect on these bonds; when Sb_4 ring is located between two In-filled voids (**Fig. 13 b**) charge depletion is clearly visible for all Sb-Sb bonds. When observing changes of Sb-Sb bond lengths it seems to be apparent that they are related to charge transfer between In and Co-Sb host structure. Presence of indium influences Sb-Sb bonds so they elongate due to the charge depletion. This small distention of Sb_4 rings cannot be assigned to a steric effect of In presence in void – in such case longer Sb-Sb bond would shrink rather than stretch.

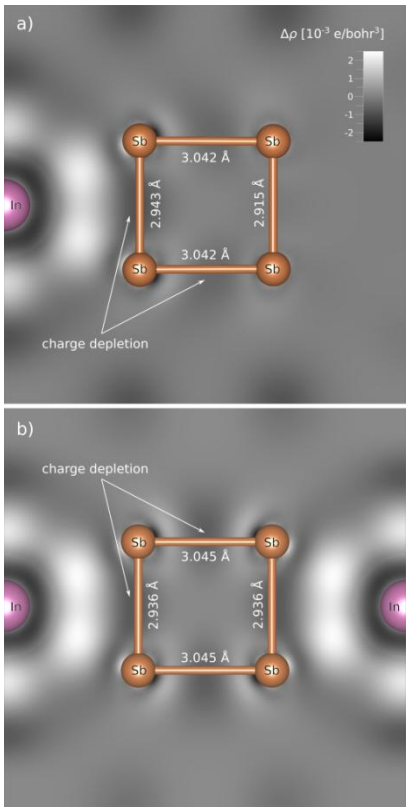

Fig. 13 Differential charge density projected on Sb_4 plane in $In_{0.75}Co_4Sb_{12}$ structure. Differential charge density was calculated as a difference between electron density distribution in $In_{0.75}Co_4Sb_{12}$ and a sum of separated In and $CoSb_3$ structures, without changing atomic positions: $\Delta\rho = \rho_{In0.75Co4Sb12} - (\rho_{Co4Sb12} + \rho_{In0.75})$.

In order to qualitatively describe local changes in topological atoms, net charges in the **Fig. 14** supercell of partially filled $In_{0.125}Co_4Sb_{12}$ has been presented, with individual atoms colored according to their net charge. Generally, in $In_xCo_4Sb_{12}$ indium atoms are positively charged (ca. 0.5 e) and play a role of a cation in the structure, transferring

some of their charges to neighboring $CoSb_6$ octahedra. At the same time Co atoms exhibit distinct negative values of net charge. The distribution of charge in individual antimony atoms is much more complex. Depending on a position in a structure they exhibit net charges between small positive value to close to zero, or even small negative ones. Almost neutral Sb atoms belong to $CoSb_6$ octahedra surrounding In-filled voids.

Theoretically calculated net charges presented in this work are contrary to former reports [46], however they strongly correlate with experimental results of XPS measurements: increasing content of indium results in a significant decrease of a binding energy of core states of Sb and Co atoms (as an effect of charge transfer from In to $CoSb_6$ octahedra). Similar change in the case of In $3d_{5/2}$ is also observed, what is consistent with theoretical analysis (for $x = 0.25$ in $In_xCo_4Sb_{12}$ $q_{In} = 0.51$ e, while for $x = 0.75$ and 1, net charge of indium topological atoms was 0.48 and 0.40 e, respectively). The greater amount of In is introduced to $CoSb_3$ voids the higher is the charge saturation of $CoSb_6$ octahedra which results in reduced effectiveness of electron extraction from filling agent.

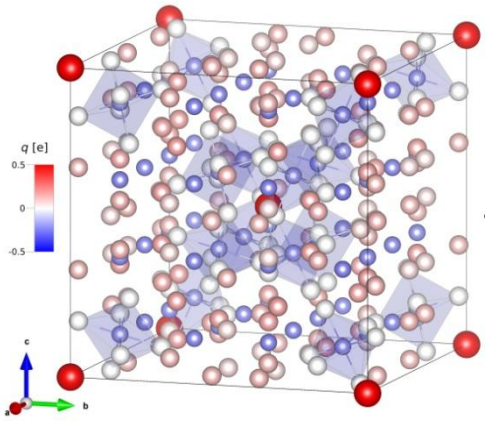

Fig. 14 Net charges of topological atoms in $In_{0.125}Co_4Sb_{12}$. Atoms colored in red have positive value of net charge and blue atoms have negative net charge value, according to the scale presented on the left. $CoSb_6$ octahedra in the immediate vicinity of In atoms have been highlighted.

Conclusions

We have successfully synthesized material with skutterudite structure using HPHT conditions. The In filing fraction determined from XRD experiments (x = 0.78) is significantly higher than the ambient pressure filling fraction limit x = 0.26 [10]. Beside the dominant skutterudite phase we observed also small amounts of $CoSb_2$, InSb and In. The observed chemical shifts in the XPS study suggest that for the In guest atoms +1 oxidation state can be assigned, while for Co and Sb the most probable oxidation states are -1 and +3, respectively.

DFT calculations of electronic structure of $In_xCo_4Sb_{12}$ using both PBE and mBJ potentials indicate change in band gap character from direct (Γ) to indirect (Γ-H) with increasing *x* what results in much higher effective mass of conducting electrons. Simultaneously, mBJ calculations show strong decrease of a band gap to 97 meV in $InCo_4Sb_{12}$. Such a small gap results in significant generation of minority carriers which can be responsible for the observed low temperature dependence of transport properties of $InCo_4Sb_{12}$ (*e.g.* resistivity decrease above 150 K).

QTAiM analysis of total electron density topology of structures with various indium amounts shows only small changes in properties of bonds, mainly related to lattice parameter changes. The In-Sb bonding is much weaker than any other bond, also presence of indium in neighborhood of Sb_4 rings affects only slightly electron density distribution around them (what results in their distention). This indicates that guest atoms have pronounced freedom of movement, leading to decrease of lattice thermal conductivity, what is clearly observed in experimental measurements.

Calculated charges of topological atoms allow us to undoubtedly define role of cobalt as anion and indium as cation, while charge of Sb atoms is varying depending on their local surrounding. The greater amount of In introduced to $CoSb_3$ the smaller is charge of indium atoms, what explains well results of XPS measurements.

HPHT synthesis route is effective method for increase of the In-filling fraction in $CoSb_3$. Increased In content resulted in much higher carrier concentration in $InCo_4Sb_{12}$ compared to $In_{0.4}Co_4Sb_{12}$, and lower absolute value of the Seebeck coefficient. Unfortunately for the thermoelectric properties, high pressure synthesis caused strong reduction of the charge carrier mobility and led to huge resistivity increase which has no justification in the DFT calculations and we link it with high pressure effects induced in the material. Increased In filling fraction yielded lower thermal conductivity as it was suggested from theory. However, keeping in mind thermoelectric performance of the material, the decrease of thermal conductivity cannot compensate for the decrease of the Seebeck coefficient and increase of resistivity. We believe that relaxation of these high pressure effects together with appropriate In filling (or other filler element) of the structural voids can improve thermoelectric properties of the *n*-type $CoSb_3$ in the temperature range where diffusion processes in this material, which can lead to decomposition, are practically inactive.

Acknowledgements

This research was supported by Polish National Science Center [grant no. 2016/21/B/ST8/00409] and in part by PL-Grid Infrastructure. The authors would like to thank prof. K. Wojciechowski for discussion, prof. L. Jaworska for HPHT experiments and prof. K. Kowalski for XPS measurements.

References

[1] V.V. Khovaylo, T.A. Korolkov, A.I. Voronin, M.V. Gorshenkov, A.T. Burkov, Rapid preparation of $In_xCo_4Sb_{12}$ with a record-breaking ZT = 1.5: the role of the In overfilling fraction limit and Sb overstoichiometry, *J. Mater. Chem. A*. **5** (2017) 3541–3546. doi:10.1039/C6TA09092C.

[2] L. Hammerschmidt, S. Schlecht, B. Paulus, Electronic structure and the ground-state properties of cobalt antimonide skutterudites: Revisited with different theoretical methods, *Phys. Status Solidi.* **210** (2013) 131–139. doi:10.1002/pssa.201228453.

[3] D. Jung, M. Whangbo, S. Alvarez, Importance of the X_4 Ring Orbitals for the Semiconducting, Metallic, or Superconducting Properties of Skutterudites MX_3 and RM_4X_{12}, *Inorg. Chem.* **29** (1990) 2252–2255. doi:10.1021/ic00337a015.

[4] J. Sofo, G. Mahan, Electronic structure of $CoSb_3$: A narrow-band-gap semiconductor, *Phys. Rev. B.* **58** (1998) 15620–15623. doi:10.1103/PhysRevB.58.15620.

[5] A. Koleżyński, W. Szczypka, Towards band gap engineering in skutterudites: The role of X_4 rings geometry in $CoSb_3$-$RhSb_3$ system, *J. Alloys Compd.* **691** (2017) 299–307. doi:10.1016/j.jallcom.2016.08.235.

[6] B. Khan, H.A.R. Aliabad, Saifullah, S. Jalali-Asadabadi, I. Khan, I. Ahmad, Electronic band structures of binary skutterudites, *J. Alloys Compd.* **647** (2015) 364–368. doi:10.1016/j.jallcom.2015.06.018.

[7] F. Tran, P. Blaha, Accurate Band Gaps of Semiconductors and Insulators with a Semilocal Exchange-Correlation Potential, *Phys. Rev. Lett.* **102** (2009) 226401. doi:10.1103/PhysRevLett.102.226401.

[8] L. Hammerschmidt, B. Paulus, Electronic structure and transport properties of filled $CoSb_3$ skutterudites by first principles, *Phys. Status Solidi.* **213** (2016) 750–757. doi:10.1002/pssa.201532609.

[9] W. Zhao, P. Wei, Q. Zhang, C. Dong, L. Liu, X. Tang, Enhanced Thermoelectric Performance in Barium and Indium Double-Filled Skutterudite Bulk Materials via Orbital Hybridization Induced by Indium Filler, *J. Am. Chem. Soc.* **131** (2009) 3713–3720. doi:10.1021/ja8089334.

[10] J. Leszczynski, V. Da Ros, B. Lenoir, A. Dauscher, C. Candolfi, P. Masschelein, J. Hejtmanek, K. Kutorasinski, J. Tobola, R.I. Smith, C. Stiewe, E. Müller, Electronic band structure, magnetic, transport and thermodynamic properties of In-filled skutterudites $In_xCo_4Sb_{12}$, *J. Phys. D. Appl. Phys.* **46** (2013) 495106. doi:10.1088/0022-3727/46/49/495106.

[11] J. Yang, L. Zhang, Y. Liu, C. Chen, J. Li, D. Yu, J. He, Z. Liu, Y. Tian, B. Xu, Investigation of skutterudite $MgyCo_4Sb_{12}$: High pressure synthesis and thermoelectric properties, *J. Appl. Phys.* **113** (2013) 113703. doi:10.1063/1.4795599.

[12] C. Sekine, H. Kato, Y. Kawamura, C.H. Lee, High-Pressure Synthesis of Skutterudite-Type Thermoelectric Materials, *Mater. Sci. Forum.* **879** (2016) 1737–1742. doi:10.4028/www.scientific.net/MSF.879.1737.

[13] X. Li, Q. Zhang, Y. Kang, C. Chen, L. Zhang, D. Yu, Y. Tian, B. Xu, High pressure synthesized Ca-filled $CoSb_3$ skutterudites with enhanced thermoelectric properties, *J. Alloys Compd.* **677** (2016) 61–65. doi:10.1016/j.jallcom.2016.03.239.

[14] X. Li, Y. Kang, C. Chen, J. Li, L. Zhang, F. Yu, D. Yu, Y. Tian, B. Xu, Thermoelectric properties of high pressure synthesized lithium and calcium double-filled $CoSb_3$, *AIP Adv.* **7** (2017) 15204. doi:10.1063/1.4974501.

[15] Q. Zhang, X. Li, Y. Kang, L. Zhang, D. Yu, J. He, Z. Liu, Y. Tian, B. Xu, High pressure synthesis of Te-doped $CoSb_3$ with enhanced thermoelectric performance, *J. Mater. Sci. Mater. Electron.* **26** (2015) 385–391. doi:10.1007/s10854-014-2411-3.

[16] J. Dong, K. Yang, B. Xu, L. Zhang, Q. Zhang, Y. Tian, Structure and thermoelectric properties of Se- and Se/Te-doped $CoSb_3$ skutterudites synthesized by high-pressure technique, *J. Alloys Compd.* **647** (2015) 295–302. doi:10.1016/j.jallcom.2015.05.171.

[17] H. Sun, X. Jia, L. Deng, P. Lv, X. Guo, Y. Zhang, B. Sun, B. Liu, H. Ma, Effect of HPHT processing on the structure and thermoelectric properties of Co_4Sb_{12} co-doped with Te and Sn, *J. Mater. Chem. A.* **3** (2015) 4637–4641. doi:10.1039/C4TA05477F.

[18] N. Dong, X. Jia, T.C. Su, F.R. Yu, Y.J. Tian, Y.P. Jiang, L. Deng, H.A. Ma, HPHT synthesis and thermoelectric properties of $CoSb_3$ and $Fe_{0.6}Co_{3.4}Sb_{12}$ skutterudites, *J. Alloys Compd.* **480** (2009) 882–884. doi:10.1016/j.jallcom.2009.02.070.

[19] L. Deng, X.P. Jia, T.C. Su, K. Jie, X. Guo, H.A. Ma, The thermoelectric properties of $In_{0.5}Co_4Sb_{12-x}Ge_x$ alloys prepared by HPHT, *Mater. Lett.* **68** (2012) 314–316. doi:10.1016/j.matlet.2011.10.035.

[20] L. Deng, L. Bin Wang, J.M. Qin, T. Zheng, X.P. Jia, H.A. Ma, Effects of indium-filling and synthesis pressure on the thermoelectric properties of $CoSb_3$, *Mod. Phys. Lett. B.* **28** (2014) 1450118. doi:10.1142/S0217984914501188.

[21] P. Blaha, K. Schwarz, G. K. H. Madsen, D. Kvasnicka and J. Luitz. WIEN2k, An Augmented Plane Wave + Local Orbitals Program for Calculating Crystal Properties. Wien: Karlheinz Schwarz, Techn. Universit ät Wien., 2001, ISBN 3-9501031-1-2.

[22] R. G. Parr and W. Yang, Density-Functional Theory of Atoms and Molecules. New York: Oxford University Press, 1989.

[23] E. Wimmer, H. Krakauer, M. Weinert, A.J. Freeman, Full-potential self-consistent linearized-augmented-plane-wave method for calculating the electronic structure of molecules and surfaces: O_2 molecule, *Phys. Rev. B.* **24** (1981) 864–875. doi:10.1103/PhysRevB.24.864.

[24] D. J. Singh. Planewaves, Pseudopotentials and the LAPW Method. Dordrecht: Kluwer Academic Publishers; 1994.

[25] J.P. Perdew, K. Burke, M. Ernzerhof, Generalized Gradient Approximation Made Simple, *Phys. Rev. Lett.* **77** (1996) 3865–3868. doi:10.1103/PhysRevLett.77.3865.

[26] M.I. Aroyo, J.M. Perez-Mato, C. Capillas, E. Kroumova, S. Ivantchev, G. Madariaga, A. Kirov, H. Wondratschek, Bilbao Crystallographic Server: I. Databases and crystallographic computing programs, *Zeitschrift Fur Krist.* **221** (2006) 15–27. doi:10.1524/zkri.2006.221.1.15; M.I. Aroyo, A. Kirov, C. Capillas, J.M. Perez-Mato, H. Wondratschek, Bilbao Crystallographic Server. II. Representations of crystallographic point groups and space groups, *Acta Crystallogr. Sect. A Found. Crystallogr.* **62** (2006) 115–128. doi:10.1107/S0108767305040286.

[27] G.K.H. Madsen, D.J. Singh, BoltzTraP. A code for calculating band-structure dependent quantities, *Comput. Phys. Commun.* **175** (2006) 67–71. doi:10.1016/j.cpc.2006.03.007.

[28] R. F. W. Bader. Atoms in Molecules: A Quantum Theory. Oxford: Clarendon Press; 1990.

[29] A. Otero-De-La-Roza, E.R. Johnson, V. Luaña, Critic2: A program for real-space analysis of quantum chemical interactions in solids, *Comput. Phys. Commun.* **185** (2014) 1007–1018. doi:10.1016/j.cpc.2013.10.026.

[30] E. Visnow, C.P. Heinrich, A. Schmitz, J. de Boor, P. Leidich, B. Klobes, R.P. Hermann, W.E. Müller, W. Tremel, On the True Indium Content of In-Filled Skutterudites, *Inorg. Chem.* **54** (2015) 7818–7827. doi:10.1021/acs.inorgchem.5b00799.

[31] K.T. Wojciechowski, J. Toboła, J. Leszczyński, Thermoelectric properties and electronic structure of $CoSb_3$ doped with Se and Te, *J. Alloys Compd.* **361** (2003) 19–27. doi:10.1016/S0925-8388(03)00411-0.

[32] G. Rogl, A. Grytsiv, P. Rogl, N. Peranio, E. Bauer, M. Zehetbauer, O. Eibl, *n*-Type skutterudites $(R,Ba,Yb)_yCo_4Sb_{12}$ (R=Sr, La, Mm, DD, SrMm, SrDD) approaching ZT≈2.0, *Acta Mater.* **63** (2014) 30–43. doi:10.1016/j.actamat.2013.09.039.

[33] G. Rogl, Z. Aabdin, E. Schafler, J. Horky, D. Setman, M. Zehetbauer, M. Kriegisch, O. Eibl, A. Grytsiv, E. Bauer, M. Reinecker, W. Schranz, P. Rogl, Effect of HPT processing on the structure, thermoelectric and mechanical properties of $Sr_{0.07}Ba_{0.07}Yb_{0.07}Co_4Sb_{12}$, *J. Alloys Compd.* **537** (2012) 183–189. doi:10.1016/j.jallcom.2012.05.011.

[34] Y.Z. Pei, L.D. Chen, W. Zhang, X. Shi, S.Q. Bai, X.Y. Zhao, Z.G. Mei, X.Y. Li, Synthesis and thermoelectric properties of $K_yCo_4Sb_{12}$, *Appl. Phys. Lett.* **89** (2006) 221107. doi:10.1063/1.2397538.

[35] X.Y. Zhao, X. Shi, L.D. Chen, W.Q. Zhang, W.B. Zhang, Y.Z. Pei, Synthesis and thermoelectric properties of Sr-filled skutterudite $Sr_yCo_4Sb_{12}$, *J. Appl. Phys.* **99** (2006) 53711. doi:10.1063/1.2172705.

[36] L.D. Chen, T. Kawahara, X.F. Tang, T. Goto, T. Hirai, J.S. Dyck, W. Chen, C. Uher, Anomalous barium filling fraction and *n*-type thermoelectric performance of $Ba_yCo_4Sb_{12}$, *J. Appl. Phys.* **90** (2001) 1864–1868. doi:10.1063/1.1388162.

[37] W. Zhao, P. Wei, Q. Zhang, H. Peng, W. Zhu, D. Tang, J. Yu, H. Zhou, Z. Liu, X. Mu, D. He, J. Li, C. Wang, X. Tang, J. Yang, Multi-localization transport behaviour in bulk thermoelectric materials, *Nat. Commun.* **6** (2015) 6197. doi:10.1038/ncomms7197.

[38] X. Tang, H. LI, Q. Zhang, M. Niino, T. Goto, Synthesis and thermoelectric properties of double-atom-filled skutterudite compounds $Ca_mCe_nFe_xCo_{4-x}Sb_{12}$, *J. Appl. Phys.* **100** (2006) 123702. doi:10.1063/1.2375017.

[39] M. Puyet, A. Dauscher, B. Lenoir, C. Bellouard, C. Stiewe, E. Müller, J. Hejtmanek, J. Tobola, Influence of Ni on the thermoelectric properties of the partially filled calcium skutterudites $Ca_yCo_{4-x}Ni_xSb_{12}$, *Phys. Rev. B.* **75** (2007) 245110. doi:10.1103/PhysRevB.75.245110.

[40] W. Schnelle, A. Leithe-Jasper, H. Rosner, R. Cardoso-Gil, R. Gumeniuk, D. Trots, J.A. Mydosh, Y. Grin, Magnetic, thermal, and electronic properties of iron-antimony filled skutterudites MFe_4Sb_{12} (M = Na,K,Ca,Sr,Ba,La,Yb), *Phys. Rev. B.* **77** (2008) 94421. doi:10.1103/PhysRevB.77.094421.

[41] P. Nieroda, J. Leszczynski, A. Kolezynski, Bismuth doped Mg2Si with improved homogeneity: Synthesis, characterization and optimization of thermoelectric properties, *J. Phys. Chem. Solids.* **103** (2017) 147–159. doi:10.1016/j.jpcs.2016.11.027.

[42] M. Puyet, B. Lenoir, A. Dauscher, C. Candolfi, J. Hejtmanek, C. Stiewe, E. Müller, Influence of Ni impurities on the thermoelectric properties of Ca-partially filled skutterudites $Ca_xCo_4Sb_{12}$, *Appl. Phys. Lett.* **101** (2012) 222105. doi:10.1063/1.4768439.

[43] D. Guo, C. Hu, Y. Xi, K. Zhang, Strain effects to optimize thermoelectric properties of doped Bi_2O_2Se via tran-blaha modified Becke-Johnson density functional theory, *J. Phys. Chem. C.* **117** (2013). doi:10.1021/jp4080465.

[44] P. Poopanya, A. Yangthaisong, Full potential calculation of electronics and thermoelectric properties of doped Mg_2Si, in: AIP Conf. Proc., 2013: pp. 415–416. doi:10.1063/1.4848462.

[45] J. Sun, D.J. Singh, Thermoelectric properties of *n*-type $SrTiO_3$, *APL Mater.* **4** (2016) 104803. doi:10.1063/1.4952610.

[46] C. Gatti, P. Macchi, Modern charge-density analysis, Springer Science & Business Media, 2012. doi:10.1007/978-90-481-3836-4.

Highlights

- HPHT synthesis allows to obtain $In_xCo_4Sb_{12}$ with x as high as 0.78.
- +1, -1 and +3 oxidation states are proposed for In, Co and Sb, respectively.
- Band gap changes from direct (Γ) to indirect (Γ-H) with increasing In content.
- DFT calculations show band gap energy decrease with increasing In content.
- HPHT synthesis reduce charge carrier mobility and leads to resistivity increase.

Table1

Table 1 Rietveld refinement of powder XRD for $InCo_4Sb_{12}$ HPHT sample.

Rietveld refinement goodness of fit parameters:						
	R_p: 32.6	R_{wp}: 21.6	R_e: 18.4	Chi^2: 1.379		
Atom	Wyckoff position	x	y	z	B_{iso}	site occupancy
Sb	24g	0.1583(15)	0.3363(13)	0.00000	0.49(3)	0.993(13)
Co	8c	0.25000	0.25000	0.25000	0.4(15)	1.00000
In	2a	0.00000	0.00000	0.00000	1.18(13)	0.78(12)
Lattice constant (Å) 9.11497(3)						
Quantitative analysis						
Phase	Faction(%)		Rf-factor			
$InCo_4Sb_{12}$	82.51(2.88)		5.06			
$CoSb_2$	9.62(0.29)		12			
InSb	6.36(0.16)		7.70			
In	1.51(0.07)		10.8			

Table2

Table 2 XPS measurement results for selected energy levels.

	Sample			
Energy level	$InCo_4Sb_{12}$	$In_{0.4}Co_4Sb_{12}$	InSb	In
In $3d_{5/2}$ (eV)	444.26	444.40	444.1	443.84
In $3d_{3/2}$ (eV)			451.69	451.34
In MNN (eV)	-	-	1077.22	1075.20
	-	-	1079.87	1078.00
	-	-	1085.28	1085.28
				Sb*
Sb $3d_{5/2}$ (eV)	527.19	527.48	527.17	528.21
	529.23	529.4	529.71	
Sb $3d_{3/2}$ (eV)	536.63	536.95	536.61	538.00
	538.72	539.08	539.25	
Sb MNN (eV)	1021.43	1022.65	1021.86	-
	1031.30	1031.70	1031.42	-
				Co*
Co $2p_{3/2}$ (eV)	777.39/778.77	777.88/780.31	-	777.90 – 778.3
Co $2p_{1/2}$ (eV)	792.42	792.75	-	793.3

*Energy levels for pure Sb and Co are taken from NIST database.

Table3

Table 3 Properties of total electron density at BCPs in $In_{0.25}Co_4Sb_{12}$: d – bond length [Å], $\rho(\mathbf{r})$ – electron density [e Å^{-3}], $\nabla^2\rho(\mathbf{r})$ – Laplacian of electron density [e Å^{-5}], $V(\mathbf{r})$ – potential energy density [a.u.], $H_e(\mathbf{r})$ – electronic energy density [a.u.]. Properties of Sb-Sb bonds have been distinguished between longer bonds (L) and shorter ones (S) in Sb_4 rings.

Bond	d	$\rho(\mathbf{r})$	$\nabla^2\rho(\mathbf{r})$	$V(\mathbf{r})$	$H_e(\mathbf{r})$
In-Sb	1,808	0,116	0,587	-0,031	-0,010
Sb-Sb (L)	1,608	0,304	0,038	-0,360	-0,179
Sb-Sb (S)	1,543	0,352	-0,061	-0,498	-0,245
Co-Sb	1,345	0,408	1,101	-0,388	-0,182